Cell Reports

EMG1 methyltransferase activity affects ribosome occupancy at KSHV uORFs

Graphical abstract

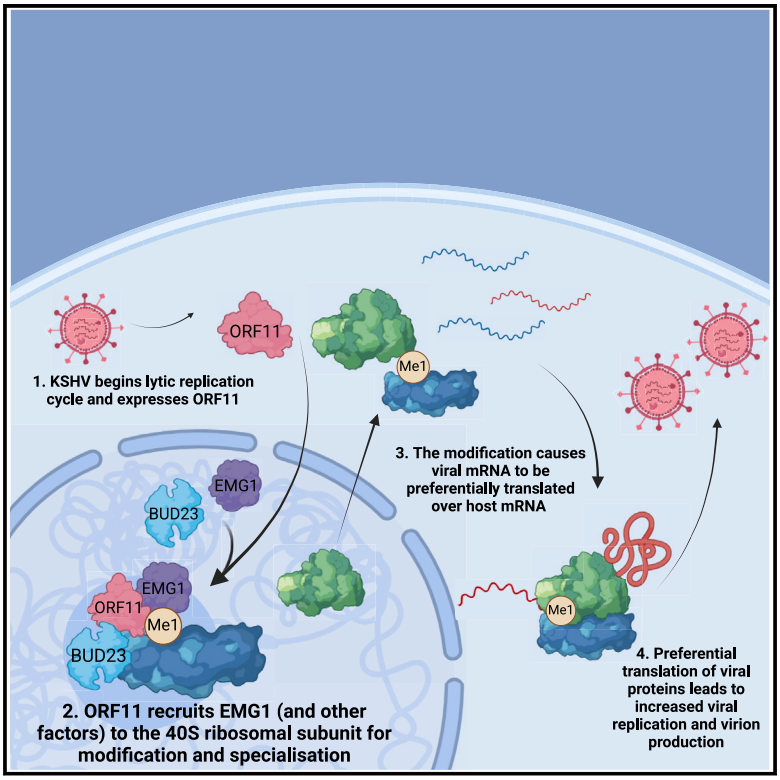

Highlights

- EMG1 has enhanced association with pre-40S ribosomal subunits during KSHV lytic replication
- Loss of EMG1 has little effect on viral mRNA levels but reduces viral protein production
- The methyltransferase activity of EMG1 results in enhanced translation of KSHV ORFs

Authors

Elena M. Harrington, James C. Murphy, Katherine L. Harper, Connor Hayward, Timothy J. Mottram, Julie L. Aspden, Adrian Whitehouse

Correspondence

a.whitehouse@leeds.ac.uk

In brief

Harrington et al. identified that the ribosomal factor EMG1 is involved in formation of specialized ribosomes during KSHV lytic replication. Its methyltransferase activity is responsible for preferential translation of KSHV ORFs. Depletion of EMG1 results in enhanced translation of KSHV uORFs, resulting in reduced viral late protein production.

Harrington et al., 2025, Cell Reports *44*, 115516
April 22, 2025
https://doi.org/10.1016/j.celrep.2025.115516

CellPress

Cell Reports

CellPress
OPEN ACCESS

Report

EMG1 methyltransferase activity affects ribosome occupancy at KSHV uORFs

Elena M. Harrington,[1,2] James C. Murphy,[1,2] Katherine L. Harper,[1,2] Connor Hayward,[1,2] Timothy J. Mottram,[1,2] Julie L. Aspden,[1,2,3] and Adrian Whitehouse[1,2,3,4,*]

[1]School of Molecular and Cellular Biology, Faculty of Biological Sciences, University of Leeds, Leeds LS2 9JT, UK
[2]Astbury Centre for Structural Molecular Biology, University of Leeds, Leeds LS2 9JT, UK
[3]LeedsOmics, University of Leeds, Leeds LS2 9JT, UK
[4]Lead contact
*Correspondence: a.whitehouse@leeds.ac.uk
https://doi.org/10.1016/j.celrep.2025.115516

SUMMARY

Viruses lack their own translational machinery and rely exclusively on the host cell for synthesis of viral proteins. Viruses have evolved diverse mechanisms to redirect the host cell translation apparatus to favor viral transcripts. A unique mechanism employed by Kaposi's sarcoma-associated herpesvirus (KSHV) involves manipulation of cellular ribosome composition, producing virus-induced specialized ribosomes. These ribosomes scan through KSHV upstream open reading frames (uORFs) in late lytic genes, allowing efficient translation of downstream main KSHV ORFs. Here, we highlight the enhanced association of the ribosomal biogenesis factor EMG1 with precursor-40S ribosome complexes during KSHV lytic replication. Depletion of EMG1 results in significantly reduced expression of viral proteins and progression through the lytic cascade, culminating in a dramatic reduction of infectious virus production. We further demonstrate that the methyltransferase activity of EMG1 is required for effective regulation of translation of KSHV uORFs in late lytic genes.

INTRODUCTION

Protein synthesis is a highly dynamic process constantly responding to changes in the environment to maintain cell homeostasis.[1,2] Historically, changes in protein synthesis were thought to be due to either gene regulation or altered characteristics of mRNAs, whereas ribosomes were considered ubiquitous, static, machine-like entities with a passive role in translation. However, emerging evidence supports an increasingly complex and dynamic network of translational regulation. Ribosome specialization offers the potential to selectively translate specific subsets of mRNAs or open reading frames (ORFs), leading to altered levels of protein expression and distinct phenotypes across cell and tissue types.[3,4] Mechanisms leading to heterogeneous populations of ribosomes within the cell can involve changes in ribosomal protein stoichiometry,[5] paralog switching,[6] post-translational modifications,[7] addition of ribosome-associated proteins,[8,9] and changes in rRNA genetic variation and modifications.[10] Evidence of specialized ribosomes is now being uncovered in differing tissue types and developmental stages or due to environmental factors such as stress, temperature, and infection.[3] This is further highlighted in ribosomopathies, a group of diseases caused by mutations or loss of ribosomal proteins and biogenesis factors that lead to reduced or altered ribosome functioning.[11]

The rapidly developing concept of specialized ribosomes poses the intriguing question of whether viruses co-opt this cellular mechanism to enhance translation of their own mRNAs. Viruses lack their own translational machinery, relying on host ribosomes to synthesize their proteins. Therefore, viruses have evolved diverse mechanisms to ensure translational efficiency of viral mRNA above and beyond that of cellular mRNA.[12,13] These processes serve to redirect the translation apparatus to favor viral transcripts, often at the expense of the host cell.

Kaposi's sarcoma-associated herpesvirus (KSHV) is a large double-stranded DNA virus associated with Kaposi's sarcoma (KS) and two lymphoproliferative disorders: multicentric Castleman disease and primary effusion lymphoma.[14,15] KSHV, like all herpesviruses, exhibits a biphasic life cycle encompassing latent persistence and lytic replication.[16] During latency, the virus remains transcriptionally dormant, with expression limited to a few latent genes, enabling long-term persistence of the viral episome.[17] Under various stimuli, the KSHV episomes are reactivated into lytic replication, leading to the ordered expression of over 80 viral proteins, culminating in the production of infectious virions.[18] This dramatic shift in viral gene expression during lytic replication from the relative dormancy of latency puts a high demand on the cellular translational machinery, and one way in which KSHV circumvents this issue is by producing specialized virus-specific ribosomes that preferentially translate viral mRNAs.[19] Quantitative proteomic affinity pull-down has previously identified changes in the stoichiometry and composition of pre-40S ribosomal complexes between latent and lytic KSHV replication cycles. Analysis identified two ribosomal

complexes that have increased association with the pre-40S ribosomal subunit during lytic KSHV replication: BUD23-TRMT112 and NOC4L-NOP14-EMG1. In addition, ribosome profiling has shown that these virus-induced specialized ribosomes reduce the translation of specific uORFs present in KSHV late lytic transcripts, which, in turn, enhances the translation of the downstream CDSs.[19] Interestingly, both the BUD23-TRMT112 and NOC4L-NOP14-EMG1 complexes contain methyltransferases, which methylate specific residues on the 18S rRNA. BUD23 mediates the N^7 methylation of 1639G,[20] whereas EMG1 catalyzes the N^1 methylation of 1248Ψ.[21] Notably, both BUD23 and EMG1 also have additional roles in ribosome biogenesis, acting as assembly scaffold proteins.[22,23]

Here, we aimed to examine the specific role of EMG1 in virus-induced specialized ribosome function. We show enhanced association of EMG1 with the pre-40S ribosomal subunit during KSHV lytic replication, resulting in a modest increase in total cellular 18S rRNA 1248 $m^1acp^3\Psi$ (1-methyl-3-α-amino-α-carboxyl-propyl pseudouridine) modification.[24] We also confirm that EMG1 is essential for KSHV lytic replication and infectious virion production. Importantly, we demonstrate that the methyltransferase activity of EMG1 is necessary for reduced occupancy at KSHV uORFs, allowing enhanced translation of the downstream viral CDS. This provides evidence that modification of rRNA can affect the activity of ribosomes during infection.

RESULTS

EMG1 has increased association with the pre-40S ribosomal subunit during KSHV lytic replication

We have previously characterized the changes to the pre-40S ribosomal subunit during the course of KSHV lytic replication by generating overexpression cell lines of FLAG-2xStrep-tagged ribosomal biogenesis proteins.[19] Specifically, DIMT1, PNO1, TSR1, and LTV1 were selected as the bait proteins due to their temporal and spatial distribution across pre-40S ribosomal subunit biogenesis and nuclear maturation. Co-immunoprecipitation coupled with quantitative mass spectrometry was performed in cells harboring latent KSHV or 24 h post induction of lytic replication, and changes in protein interactions between the two conditions were assessed. The NOC4L-NOP14-EMG1 complex was shown to have substantially increased stoichiometry with pre-40S complexes during KSHV lytic compared to latent replication cycles. EMG1 is the methyltransferase within the complex that catalyzes the N^1 methylation of Ψ1248 residues on the 18S rRNA.[21] Therefore, we aimed to determine whether the catalytic activity of EMG1 is required for KSHV-mediated specialized ribosome function.

To first confirm an increased association between EMG1 and the pre-40S ribosomal subunit during KSHV lytic replication, FLAG affinity pulldown was performed, using one of the bait protein cells lines used previously in the quantitative pull-down (TREx-BCBL1-Rta cells stably expressing FLAG-2xStrep-PNO1), during latent and lytic replication phases. PNO1 is an essential ribosome biogenesis protein that binds pre-40S complexes before nuclear export and aids in structural configuration of the subunit during both nuclear and cytoplasmic maturation.[25] Immunoblot analysis confirmed a 3-fold increase in association between EMG1 and PNO1 during KSHV lytic replication compared with cells harboring latent KSHV, while no change in association was observed in the control core ribosomal protein eS19, confirming the previous quantitative proteomics results (Figure 1A). To confirm that these results were not due to the artificial doxycycline-induced reaction system of TREx-BCBL1-Rta cells, native PNO1 pulldown was also performed in BCBL1 cells reactivated with sodium butyrate and tetradecanoyl phorbol acetate (TPA) (Figure S1). Once again, PNO1 had an increased association with EMG1 (3.8-fold) during lytic KSHV replication compared to cells harboring latent KSHV. Previous research has identified the viral protein ORF11 as the mediator for specialized ribosomes during lytic replication[19]; therefore, the association between EMG1 and ORF11 was probed via FLAG co-immunoprecipitation in the TREx-BCBL-Rta FLAG-ORF11 overexpression cell line (Figure 1B). ORF11 associates with EMG1 during both latent and 24 h lytic conditions. ORF11 is not expressed during latency and is only present due to the overexpression construct; however, this interaction in latency suggests that ORF11 does not require other lytically expressed factors to bind with ribosomal factors. However, the 2- to 3.5-fold increase in association with EMG1/NOC4L/NOP14 during lytic replication suggests that other viral factors may enhance this interaction.

Surprisingly, while EMG1 has an enhanced association with the pre-40S during KSHV lytic replication, EMG1 mRNA levels are reduced by 40%, whereas EMG1 protein levels remain stable after 24 h of lytic replication (Figures 1C and 1D), suggesting that the increased association of EMG1 is directly driven by the virus at early stages of replication. EMG1 methylates base 1248 of the 18S rRNA within a three-part modification, which also includes pseudouridinylation and the addition of an acp moiety.[24] While the methylation cannot be investigated in isolation, an aminocarboxyl propyl reverse-transcription PCR (aRT-PCR) assay has been developed that measures 18S rRNA 1248$m^1acp^3\Psi$ modification.[24] Upon KSHV reactivation, a decrease in total cellular unmodified 18S rRNA 1248U is observed, from 18% to 8% after 48 h of lytic replication (Figure 1E), which suggests that the increased association of EMG1 increases 18S rRNA 1248$m^1acp^3\Psi$ modification. This leads to an increase in modified ribosomes from 82% to 92% during KSHV lytic replication. Polysome profiling was also utilized to isolate 40S ribosomal subunits, and then the levels of 18S rRNA 1248$m^1acp^3\Psi$ modification were analyzed. Interestingly, there was a larger change in unmodified 18S rRNA 1248U after 24 h of lytic replication (7% unmodified) compared to cells harboring latent KSHV (33% unmodified) (Figure 1F), confirming an increase in modified ribosomes from 67% to 93% during KSHV lytic replication. Overall, this shows a modest increase in total cellular 18S rRNA 1248 $m^1acp^3\Psi$ modification during lytic replication, which is seen to a greater extent in isolated 40S ribosomal subunits. Overall, the results suggest that KSHV enhances the association between EMG1 and pre-40S during ribosomal biogenesis in the early stages of lytic replication, resulting in a modest increase in 18S rRNA 1248$m^1acp^3\Psi$ modification in 40S ribosomal subunits.

EMG1 is essential for efficient KSHV lytic replication

To determine whether the increased association of EMG1 with the pre-40S subunit is important for KSHV lytic replication,

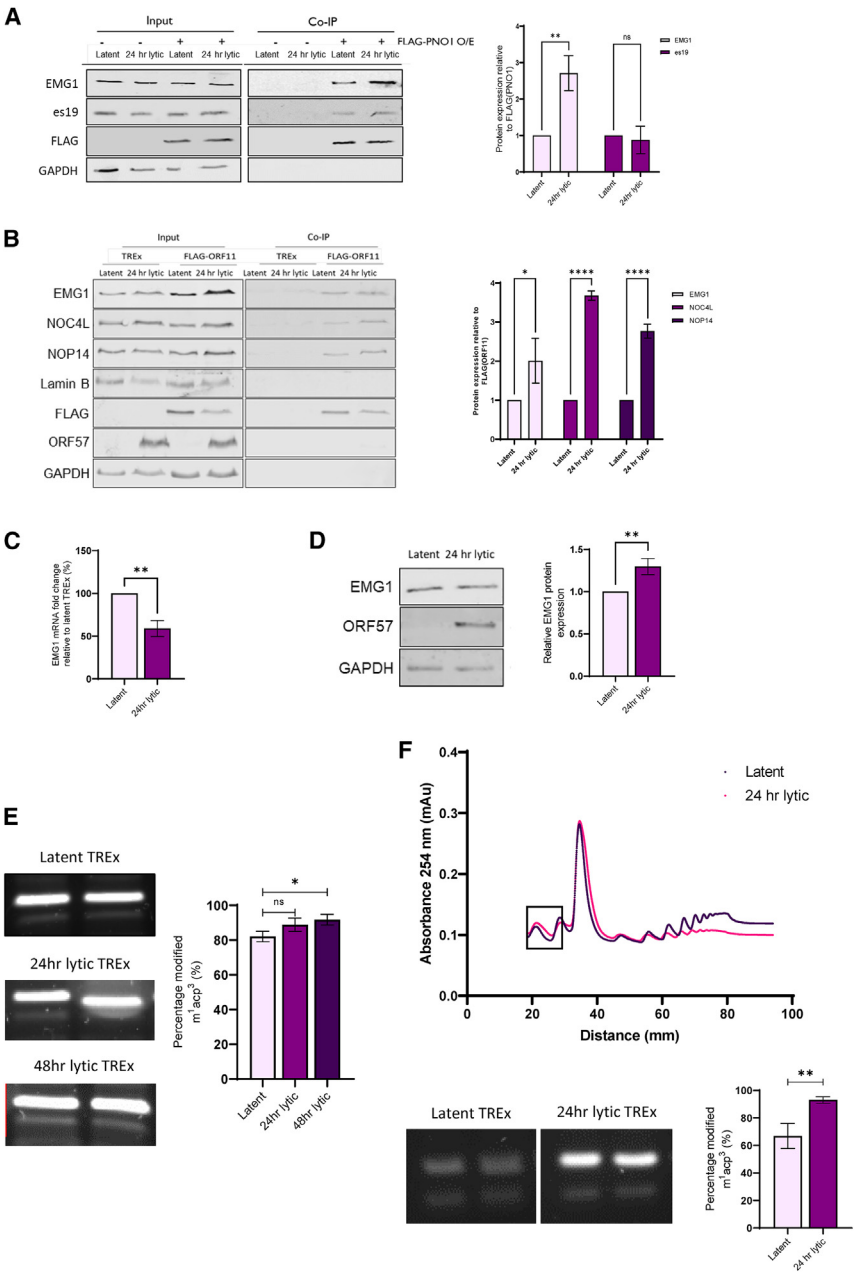

Figure 1. Increased association of EMG1 with pre-40S complexes during KSHV lytic replication

(A and B) TREx-BCBL1-Rta cells stably expressing a FLAG-PNO1 overexpression construct or wild-type TREx-BCBL1-Rta cells were induced for KSHV lytic replication for 24 h or remained latent.

(A) FLAG(PNO1) trap elution was performed on the whole-cell lysates and probed via immunoblotting alongside the whole-cell lysate inputs with EMG1, FLAG, eS19, and GAPDH antibodies ($n = 3$). Shown is densitometry analysis of the FLAG trap pulldown normalized to the levels of the bait protein PNO1 (FLAG). Unpaired, two-tailed Student's t test was used ($n = 3$).

(B) FLAG(ORF11) trap elution was performed on the whole-cell lysates and probed via immunoblotting alongside the whole-cell lysate inputs with EMG1, NOC4L, NOP14, Lamin B, FLAG, ORF57, and GAPDH antibodies ($n = 3$). Shown is densitometry analysis of the FLAG trap pulldown normalized to the levels of the bait protein ORF11(FLAG). Unpaired, two-tailed Student's t test was used ($n = 3$).

(C and D) TREx-BCBL1-Rta cells were reactivated for 24 h or remained latent. RNA (C) and protein (D) from cell lysates were probed for EMG1 expression, normalized to GAPDH ($n = 3$). Shown is densitometry analysis of EMG1 protein expression, normalized to GAPDH. Unpaired, two-tailed Student's t test was used ($n = 3$).

(E and F) Aminocarboxyl propyl reverse-transcription PCR (aRT-PCR) was performed on (E) whole cell lysates and (F) isolated 40S ribosomal subunits via polysome profiling. Significance was calculated by one-way analysis of variance (ANOVA) (E) or unpaired, two-tailed Student's t test (F).

Data are presented as mean ± SD. Asterisks denote a significant difference between the specified groups (*$p \leq 0.05$, **$p < 0.01$, ***$p < 0.001$, and ****$p < 0.0001$).

TREx-BCBL1-Rta cells were stably transduced with lentivirus-based EMG1-targeting shRNAs, depleting EMG1 mRNA levels by 70% (KD1) and 60% (KD2) and protein levels by 98% (KD1) and 96% (KD2), respectively (Figures 2A and 2B). To confirm that depletion of a host ribosome biogenesis factor had limited effect on TREx-BCBL1-Rta cells, a series of assays measuring protein turnover, ribosome population, and translational capacity were performed, comparing the two EMG1-depleted TREx-BCBL1-Rta cell lines and a scr control. Polysome profiling (Figure 2C) was also used to compare the ribosome population, showing that levels of 80S ribosomes and polysomes upon EMG1 knockdown are similar to the control, indicating that loss of EMG1 had little effect on ribosome biogenesis or overall ribosome levels in KSHV latently infected cells (Figure 2D). The 40S ribosomal subunits were isolated, and 18S rRNA 1248$m^1acp^3\Psi$ modification was probed via an aRT-PCR assay (Figure 2E), in which both cell lines showed a modest decrease in modification compared to scr (16% and 7%, respectively). This suggests that EMG1 depletion decreases the modification efficiency from 82% to 65.6% for KD1 and 90%–83.7% for KD2. Global protein turnover was also measured, using CDK1 as a marker, with immunoblot analysis showing no significant change in CDK1 protein levels in scr shRNA-treated control cells compared to cells depleted of EMG1 (Figure 2F). Finally, EMG1 depletion had no significant effect on global translational output, as assayed by labeling nascent proteins with click-iT L-azidohomoalanine and quantifying by flow cytometry (Figure 2G). Based on these assays, no significant adverse effects on TREx-BCBL1-Rta ribosome

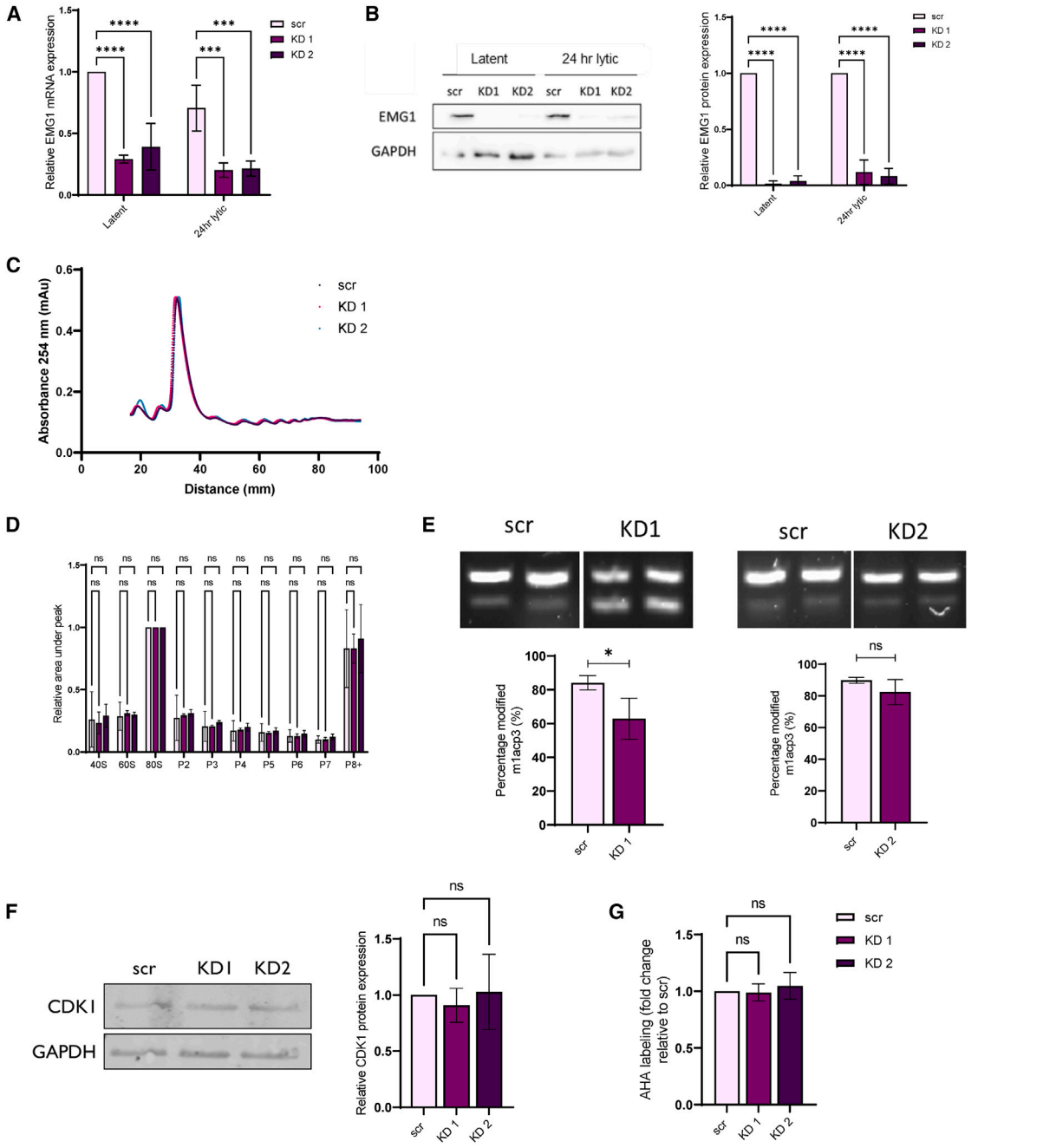

Figure 2. EMG1 depletion does not affect global translation in KSHV-infected TREx-BCBL1-Rta cells

(A and B) TREx-BCBL1-Rta cells containing shRNAs targeting EMG1 or a scr shRNA were used to study the effects of EMG1 depletion. Shown are mRNA (A) and protein (B) expression of EMG1 in EMG1-depleted TREx-BCBL1-Rta cells compared to the scr control during latent and lytic KSHV replication ($n = 3$). Also shown is densitometry analysis of EMG1 protein expression in TREx-BCBL1-Rta cells depleted of EMG1 compared to the scr control, normalized to GAPDH. Significance was calculated by one-way ANOVA ($n = 3$).

(C–E) Polysome profiling traces of (C) latent TREx-BCBL1-Rta cells depleted of EMG1 or containing scr plasmid ($n = 3$) and (D) densitometry analysis of the area of each polysome fraction, measured relative to the 80S subunit. The densitometry value of each peak was measured in triplicate and averaged on each biological repeat. Significance was calculated by one-way ANOVA ($n = 3$). The 40S subunit was isolated, and aRT-PCR was performed, measuring changes in m^1acp^3 modification (E). Significance was calculated by unpaired two-tailed Student's t test ($n = 3$).

(F) Protein lysates of latent TREx-BCBL1-Rta cells depleted of EMG1 or a scr control were probed via immunoblotting with CDK1 and GAPDH antibodies ($n = 3$). Shown is densitometry analysis of CDK1 expression in EMG1-depleted cells, normalized to GAPDH. Significance was calculated by one-way ANOVA ($n = 3$).

(legend continued on next page)

population and translational capacity were observed upon EMG1 depletion.

To assess the effect of preventing the enhanced association of EMG1 with pre-40S ribosomal complexes upon KSHV lytic replication, the transcription and translation of viral early and late genes was assessed in EMG1-depleted TREx-BCBL1-Rta cell lines compared to a scr control. It would be predicted that modification of the host cell ribosome population to produce virus-induced specialized ribosomes during infection would impact late viral protein production rather than the early stages post reactivation. To this end, mRNA and protein levels of the early KSHV *ORF57* and *K8* and late *ORF26* and *ORF65* genes were compared 24 h post reactivation (Figures 3A–3D). The results showed no statistically significant decrease in mRNA expression of any of the viral gene panels. In contrast, while early ORF57 and K8 protein levels remained relatively stable 24 h post lytic induction (Figure 3E), EMG1 depletion significantly inhibited late ORF26 (53% and 35%) and ORF65 (77% and 49%) protein production 48 h post lytic induction (Figure 3F). RT-qPCR of polysome fractions was then used to observe changes in active translation of viral *ORF57* and *ORF65* transcripts upon EMG1 depletion compared to the scr control during KSHV lytic replication (Figure 3G). Highly active translating mRNAs with three or more ribosomes bound were collected, and the levels of *ORF57* and *ORF65* transcripts in these fractions were quantified. EMG1 depletion did not cause reduced translation of *ORF57* mRNA, with KD1 showing a 50% increase in polysome association and KD2 retaining stable levels of polysome association. Conversely, *ORF65* mRNA was dramatically reduced by 60% and 48% (Figure 3G), suggesting that EMG1 knockdown results in reduced translation of late viral transcripts. Interestingly, a consistent increase in mRNA expression of viral transcripts was observed, which could be due to positive feedback from the loss in protein production. It is hypothesized that KSHV increases viral mRNA expression to resolve this loss of late viral protein production.

Finally, to confirm that EMG1 depletion affected later stages of KSHV lytic replication, infectious virion production was assessed. Here, TREx-BCBL-Rta cells depleted of EMG1 or containing an scr plasmid were reactivated for 72 h. Cells were harvested, and the DNA was collected from cell pellets to assess viral load (Figure 3H), while the supernatant containing any infectious virion was introduced to naive HEK293T cells in a dose-dependent manner. Total RNA (Figure 3I) and DNA (Figure 3J) were isolated, and *ORF57* expression or genomic DNA was probed to analyze the capability of virions to re-infect naive HEK293T cells. TREx-BCBL-Rta cells depleted of EMG1 had a modest but significant reduction in viral load (Figure 3H) of 21% (KD 1) and 25% (KD 2). Upon reinfection, the presence of KSHV genomes was markedly reduced by 69% (KD 1) and 37% (KD 2) in a dose-dependent manner. The viral RNA expression corroborated this trend, with a 57% (KD 1) and 49% (KD 2) reduction in viral RNA expression relative to scr, also dose dependent. This suggests that cells depleted of EMG1 produce fewer infectious virions capable of successfully reinfecting naive cells. This was further confirmed by the almost total loss of staining for the viral marker LANA in naive HEK293T cells, which were re-infected with virus produced from cells depleted of EMG1 compared to the scr control (Figure 3K). Taken together, these results suggest that EMG1 depletion significantly reduces the translation of late viral proteins, which impacts downstream production of new infectious virions.

EMG1 methyltransferase activity affects ribosome occupancy at KSHV uORFs, impacting translation of the downstream CDS

Ribosome profiling has revealed previously that KSHV specialized ribosomes scan through viral late-gene uORFs, overcoming uORF-mediated repression and enhancing translation of the downstream viral main ORFs.[19] To determine whether EMG1 regulates ribosome occupancy at viral uORFs, dual-luciferase reporter constructs were utilized, comprising ORF28, ORF34, and ORF69 5′ UTRs, each containing a uORF shown previously to be regulated by KSHV-induced specialized ribosomes.[19] The uORF start codon of each construct has been mutated previously and resulted in increased translation of the downstream luciferase reporter, thus confirming that the uORF regulates the translation of the downstream coding sequence.[19] These 5′ UTR-luciferase reporter constructs were transfected into HEK293T cells containing a scr shRNA or shRNAs targeting EMG1. Similar to TREx-BCBL1-Rta cells, shRNA-mediated depletion resulted in efficient EMG1 knockdown of >90% (Figure 4A). Notably, EMG1 depletion significantly reduced the expression of the downstream luciferase reporter in the presence of all three 5′ UTRs: ORF28 (25% and 34%), ORF34 (50%), and ORF69 (20% and 27%) compared to the scrambled control (Figures 4B and S2).

To determine whether the reduction of luciferase activity was dependent on the methyltransferase activity of EMG1, an EMG1 mutant construct was generated that replaced the previously characterized catalytic loop (RPDI- arginine, proline, aspartate, isoleucine, residues 84–88) with alanine residues to produce a catalytically inactive EMG1 construct.[26] Two rescue cell lines were generated by expressingan shRNA-resistant construct of either a catalytically inactive mutant EMG1 (Figure 4C) or wild-type EMG1 (Figure 4E) in EMG1 shRNA-depleted cells. The ORF34 5′ UTR containing the dual-luciferase plasmid was then transfected into each cell line to assess translation regulation. The results showed that rescue of EMG1 knockdown with wild-type EMG1 alleviated this repression and upregulated downstream luciferase reporter expression compared to the scr control. In contrast, expression of the EMG1 catalytic mutant was unable to rescue the reduced luciferase expression in the presence of the KSHV 5′ UTR containing the ORF34 uORF (Figures 4D and 4F). Interestingly, TREx-BCBL1-Rta EMG1 knockdown

(G) A methionine chase experiment measured global translation by depleting methionine from the cells and then labeling nascent peptides with click-iT L-azidohomoalanine (AHA). The abundance of AHA was measured via flow cytometry using alkyne Alexa Fluor 488. Significance was calculated by one-way ANOVA ($n = 3$).

Data are presented as mean ± SD. Asterisks denote a significant difference between the specified groups (*$p \leq 0.05$, ***$p < 0.001$, and ****$p < 0.0001$).

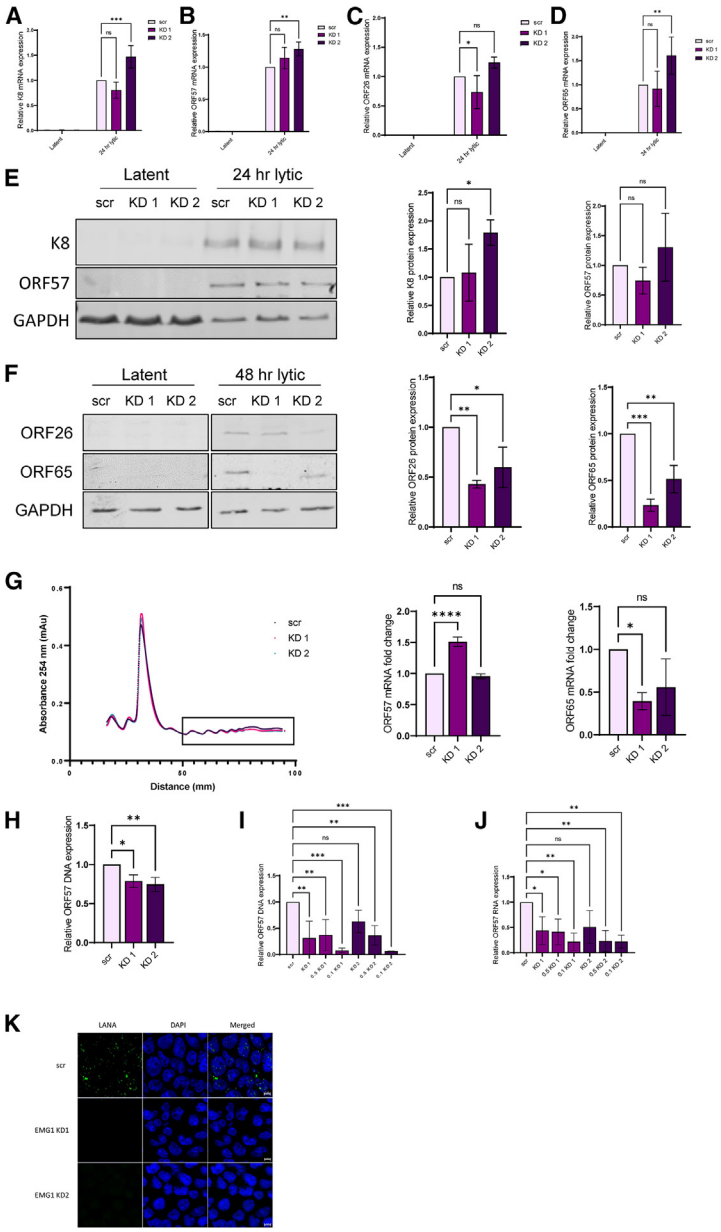

Figure 3. EMG1 is required for efficient KSHV lytic replication

(A–F) Latent and 24 h reactivated cell lysates from TREx-BCBL1-Rta cells depleted of EMG1 or a scr control were analyzed for mRNA expression of (A) *K8*, (B) *ORF57*, (C) *ORF26*, and (D) *ORF65*, normalized to *GAPDH*. Significance was calculated by one-way ANOVA ($n = 3$).

(E) ORF57 and K8 protein expression was measured in cell lysates after 24 h of lytic replication or harboring latent KSHV. Densitometry analysis of protein expression was normalized to GAPDH, and significance was calculated by one-way ANOVA ($n = 3$). (F) Protein expression of ORF26 and ORF65 was measured in cell lysates after 48 h of lytic replication or harboring latent KSHV. Densitometry analysis of protein expression was normalized to GAPDH, and significance was calculated by one-way ANOVA ($n = 3$).

(G) Polysome profiling was performed in TREx-BCBL1-Rta cells depleted of EMG1 or a scr control after 24 h KSHV lytic replication. Total RNA was isolated from traces containing 3 or more polysomes, and expression of the viral genes *ORF57* and *ORF65* was analyzed via qPCR and normalized to housekeeping genes. Significance was calculated by one-way ANOVA ($n = 3$).

(H–K) TREx-BCBL1-Rta cells depleted of EMG1 or a scr control were reactivated for 72 h DNA was isolated from cell lysates, and viral load was measured by qPCR, normalized to GAPDH (H). Significance was calculated by one-way ANOVA ($n = 3$). Supernatant containing infectious virions was introduced to naive HEK293T cells in doses of either total supernatant, 0.5-fold total, or 0.1-fold total for 48 h, and total (I) DNA and (J) RNA were isolated. *ORF57* expression was measured via qPCR, normalized to *GAPDH*. Significance was calculated by one-way ANOVA ($n = 3$).

(K) Reinfected HEK293T cells were permeabilized and stained for LANA (green) and DAPI (blue). The cells were mounted on coverslips and visualized using an inverted LSM800 confocal microscope.Data are presented as mean ± SD. Asterisks denote a significant difference between the specified groups ($*p \leq 0.05$, $**p < 0.01$, $***p < 0.001$, and $****p < 0.0001$).

cells did not decrease the level of *ORF34* mRNA (Figure S3); therefore, these changes in uORF reporter expression are not due a reduction in expression of the viral RNA transcripts. Taken together, these findings support the hypothesis that the methyltransferase activity of EMG1 enables reduced translation at KSHV uORFs, allowing enhanced translation of downstream CDSs.

DISCUSSION

Like all viruses, KSHV lacks its own translational machinery and therefore must manipulate the host cell translational apparatus to enable preferential translation of viral mRNAs over host mRNAs.[12,19] KSHV produces virus-induced specialized ribosomes by enhancing the recruitment of specific ribosomal biogenesis factors to the pre-40S ribosomal subunit during early stages of lytic infection through the activity of the KSHV ORF11 protein.[19] However, the precise role of these ribosome-associated factors has yet to be determined. A clue may lie in the complexes that have been identified: BUD23 and its co-factor TRMT112, and the NOC4L-NOP14-EMG1 complex. Interestingly, both of these complexes contain methyltransferase activities that modify the 18S rRNA. BUD23 methylates m^7-G1639, whereas EMG1 methylates N^1-1248Ψ.[20,21] However, it is unknown whether the methyltransferase activity of these complexes is essential for KSHV specialized ribosome function. Here, we demonstrate that the methyltransferase activity of EMG1 is essential to regulate KSHV-mediated specialized ribosome association with viral uORFs that regulate translation of the downstream CDSs.

Surprisingly, EMG1 was dispensable for host cell proliferation, having little effect on ribosome biogenesis or global translation in latently KSHV-infected TREx-BCBL1-Rta cells. This may suggest tissue- or cell-specific differences in the essential nature of EMG1, similar to other ribosomal biogenesis factors. This is emphasized by a single amino acid mutation (aspartate to

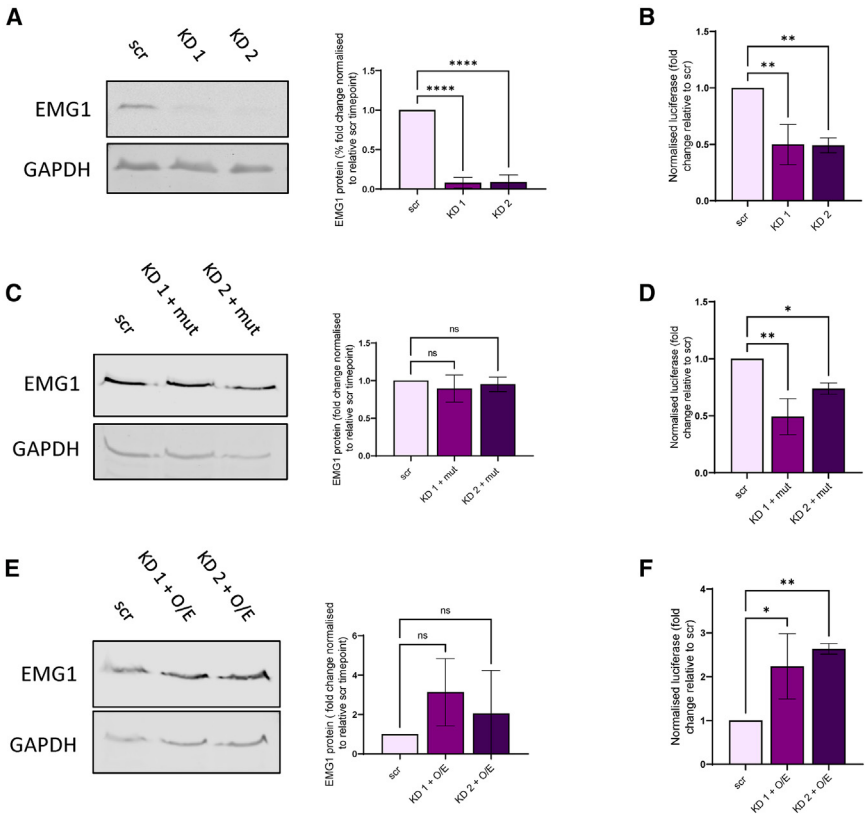

Figure 4. EMG1 methyltransferase activity is required to regulate viral uORF ribosome occupancy

Protein lysates of HEK293T cells expressing scr shRNA, (A) EMG1 shRNA, (C) catalytically inactive EMG1 (mut), or (E) wild-type EMG1 overexpression plasmids (O/E) were probed for expression of EMG1 via western blot (n = 3). Shown is densitometry analysis of EMG1 expression relative to GAPDH in varying HEK293T cell lines. Significance was calculated by one-way analysis of variance (ANOVA) (n = 3). A dual-luciferase reporter construct containing the 5′ untranslated region (UTR) of ORF34 was transfected into (B) EMG1-depleted cells, (D) EMG1-depleted cells rescued with a catalytically inactive EMG1 construct (mut), and (F) EMG1-depleted cells recovered with a wild-type EMG1 overexpression construct (O/E). Luciferase activity was normalized to the scr shRNA control cell line. Significance was calculated using one-way ANOVA (n = 3). Data are presented as mean ± SD. Asterisks denote a significant difference between the specified groups (*$p \leq 0.05$, **$p < 0.01$, ***$p < 0.001$, and ****$p < 0.0001$).

glycine) at position 86 within EMG1, associated with Bowen-Conradi syndrome.[27] This rare ribosomopathy is characterized by moderate to severe prenatal and postnatal growth retardation, microcephaly, a distinctive facial appearance, profound psychomotor delay, hip and knee contractures, and rocker bottom feet.[28] Mutation at residue 86 does not affect the methyltransferase catalytic activity but is thought to lead to its nuclear aggregation and degradation, resulting in reduced nucleolar recruitment.[29] This emphasizes the scaffolding function of EMG1, and presence within the pre-ribosomal complex is essential, whereas the N^1 methylation of Ψ1248 on the 18S rRNA is a non-essential modification. This leads to the hypothesis that the methyltransferase activity of EMG1 could be a preferential modification triggered under different conditions, serving to modify the 18S rRNA and contributing to the regulation of translation.

In contrast, EMG1 is required for efficient KSHV lytic replication and infectious virion production. Notably, EMG1 depletion had little effect on KSHV *K8*, *ORF57*, *ORF26*, and *ORF65* mRNA levels; however, translation and protein production of the late viral ORF26 and ORF65 proteins was dramatically reduced. Together, these results demonstrate that EMG1 enhances the translation of late viral proteins, resulting in the collapse of the late lytic gene cascade and culminating in dramatically reduced levels of KSHV infectious virions. As the EMG1 depletion phenotype is similar to BUD23 depletion, it is possible that both of these methyltransferases are modifying the 18S rRNA, resulting in a cumulative effect that changes which ORFs ribosomes preferentially translate. While there have been no other published examples linking viral translation and EMG1, viruses have been reported to modify ribosomes via multiple mechanisms. Therefore, it is possible that EMG1 and BUD23 enrichment at the pre-40S ribosomal subunit is not unique to KSHV and employed by other viruses as a strategy to enhance translation of viral transcripts and, ultimately, virion production.

Through ribosome profiling, we have shown previously that KSHV-induced specialized ribosomes prevent occupancy and thereby reduce translation of viral uORFs in late lytic KSHV mRNAs and, consequently, the efficient translation of the downstream CDS.[19] We therefore investigated whether EMG1, and specifically its methyltransferase activity, is involved in this regulatory mechanism. Importantly, luciferase reporter assays confirmed that EMG1 depletion resulted in a decrease in downstream CDS translation, likely due to an increase in uORF translation. Of key importance is the finding that the methyltransferase activity of EMG1 is the essential aspect for KSHV replication and infectious virion production. Notably, the 18S rRNA base 1248 has a three-part temporal modification in which it is initially pseudouridinylated, followed by Tcr adding an acp^3 modification, and finally EMG1 enables N^1 methylation.[24] The modified 1248Ψ base sits in the P site, adjacent to the codon:anti-codon interface, which suggests that these modifications are essential for allowing cognate codon:anti-codon pairings.[30] Recent dynamic simulations suggest that addition of this methyl group stabilizes the interaction of the ribosome with tRNA.[24] Therefore, without this methylation, there may be reduced restriction on codon:anti-codon pairing, allowing more non-canonical base pairing to occur and leaky codon pairings to pass through the ribosome.

In summary, we show an enhanced recruitment of EMG1 to newly synthesized ribosomes during early stages of KSHV lytic replication. This enables the production of a virally induced

specialized ribosome, which preferentially translates viral late proteins. Mechanistic studies demonstrate that the methyltransferase activity of EMG1 is required for reduced translation at KSHV uORFs, allowing enhanced translation of the downstream CDSs.

Limitations of the study

This study has identified EMG1 as a ribosomal factor involved in the formation of specialized ribosomes during KSHV lytic replication. Importantly, the aRT-PCR assay used in this study to identify changes in modification to the 18S rRNA 1248U is not specific to just the N^1 methylation. Being able to measure just the changes in the N^1 methylation would be an interesting next step in this research; however, this may require development of new technology, as methods such as direct RNA sequencing are currently unable to differentiate between the pseudouridinylation, methylation, and acp modification on the base.

The results here show a modest increase in the fraction of virus-induced modified ribosomes upon KSHV lytic replication. While this indicates a small effect on the amount of modification of the ribosome pool, it is significant enough to provide an advantage for KSHV replication. However, it may also be the case that these modified ribosomes already comprise the majority of the ribosomal particles in the cell and that the virus is just enhancing their production, although what the role the unmodified ribosomes play during infection is unclear.

Finally, we have now identified two ribosomal-associated factors involved in the formation of specialized ribosomes during KSHV lytic replication. Both of these proteins were investigated in isolation; however, future research could combine the two proteins to explore the potential combinatorial effect of several modifications on ribosomes, which is likely what is occurring during viral infection.

RESOURCE AVAILABILITY

Lead contact

Requests for further information, resources, and reagents should be directed to and will be fulfilled by the lead contact, Adrian Whitehouse (a.whitehouse@leeds.ac.uk).

Materials availability

Primary materials generated during this study are available from the lead contact upon request.

Data and code availability

- This paper does not report any original datasets or original code.
- Any additional information required to reanalyze the data reported in this paper is available from the lead contact upon request.

ACKNOWLEDGMENTS

We thank Prof. Jae Jung, University of Southern California School of Medicine, Los Angeles. This work was supported by a University of Leeds Mary & Alice Smith Endowed Research Scholarship (to E.M.H. and A.W.), the Wellcome Trust (to J.C.M. and A.W., 203826/Z/16/Z), BBSRC (to A.W.), and JLA (BB/N014405/1 and BB/X003086/1).

AUTHOR CONTRIBUTIONS

Conceptualization, E.M.H. and A.W.; data curation, E.M.H., J.C.M., K.L.H., C.H., and T.J.M.; formal analysis, E.M.H., J.C.M., K.L.H., C.H., T.J.M., J.L.A., and A.W.; funding acquisition, E.M.H., J.C.M., J.L.A., and A.W.; investigation, E.M.H. and J.C.M.; writing – original draft, E.M.H. and A.W.; writing – review & editing, all authors.

DECLARATION OF INTERESTS

The authors declare no competing interests.

STAR★METHODS

Detailed methods are provided in the online version of this paper and include the following:

- KEY RESOURCES TABLE
- EXPERIMENTAL MODEL
  - Cell culture
  - Plasmid constructs
- METHOD DETAILS
  - Co-immunoprecipitations
  - Immunoblotting
  - RNA extraction and qPCR
  - Aminocarboxyl propyl reverse transcription (aRT)-PCR assay
  - Lentiviral expression and shRNA constructs
  - Global translation assay
  - Viral load and reinfection assays
  - Immunofluorescence
  - Polysome profiling
  - Luciferase assays
- QUANTIFICATION AND STATISTICAL ANALYSIS

SUPPLEMENTAL INFORMATION

Supplemental information can be found online at https://doi.org/10.1016/j.celrep.2025.115516.

Received: June 26, 2024
Revised: January 22, 2025
Accepted: March 14, 2025
Published: April 10, 2025

REFERENCES

1. Frank, J. (2000). The ribosome–a macromolecular machine par excellence. Chem. Biol. *7*, R133–R141.
2. Hinkson, I.V., and Elias, J.E. (2011). The dynamic state of protein turnover: It's about time. Trends Cell Biol. *21*, 293–303. https://doi.org/10.1016/j.tcb.2011.02.002.
3. Genuth, N.R., and Barna, M. (2018). The Discovery of Ribosome Heterogeneity and Its Implications for Gene Regulation and Organismal Life. Mol. Cell *71*, 364–374. https://doi.org/10.1016/j.molcel.2018.07.018.
4. Xue, S., and Barna, M. (2012). Specialized ribosomes: a new frontier in gene regulation and organismal biology. Nat. Rev. Mol. Cell Biol. *13*, 355–369. https://doi.org/10.1038/nrm3359.
5. Shi, Z., Fujii, K., Kovary, K.M., Genuth, N.R., Röst, H.L., Teruel, M.N., and Barna, M. (2017). Heterogeneous Ribosomes Preferentially Translate Distinct Subpools of mRNAs Genome-wide. Mol. Cell *67*, 71–83. https://doi.org/10.1016/j.molcel.2017.05.021.
6. Hopes, T., Norris, K., Agapiou, M., McCarthy, C.G.P., Lewis, P.A., O'Connell, M.J., Fontana, J., and Aspden, J.L. (2022). Ribosome heterogeneity in Drosophila melanogaster gonads through paralog-switching. Nucleic Acids Res. *50*, 2240–2257. https://doi.org/10.1093/nar/gkab606.
7. Gupta, V., and Warner, J.R. (2014). Ribosome-omics of the human ribosome. RNA *20*, 1004–1013. https://doi.org/10.1261/rna.043653.113.
8. Simsek, D., and Barna, M. (2017). An emerging role for the ribosome as a nexus for post-translational modifications. Curr. Opin. Cell Biol. *45*, 92–101. https://doi.org/10.1016/j.ceb.2017.02.010.

9. Simsek, D., Tiu, G.C., Flynn, R.A., Byeon, G.W., Leppek, K., Xu, A.F., Chang, H.Y., and Barna, M. (2017). The Mammalian Ribo-interactome Reveals Ribosome Functional Diversity and Heterogeneity. Cell *169*, 1051–1065. https://doi.org/10.1016/j.cell.2017.05.022.

10. Roundtree, I.A., Evans, M.E., Pan, T., and He, C. (2017). Dynamic RNA Modifications in Gene Expression Regulation. Cell *169*, 1187–1200. https://doi.org/10.1016/j.cell.2017.05.045.

11. Kampen, K.R., Sulima, S.O., Vereecke, S., and De Keersmaecker, K. (2020). Hallmarks of ribosomopathies. Nucleic Acids Res. *48*, 1013–1028. https://doi.org/10.1093/nar/gkz637.

12. Stern-Ginossar, N., Thompson, S.R., Mathews, M.B., and Mohr, I. (2019). Translational Control in Virus-Infected Cells. Cold Spring Harbor Perspect. Biol. *11*, a033001. https://doi.org/10.1101/cshperspect.a033001.

13. Walsh, D., Mathews, M.B., and Mohr, I. (2013). Tinkering with translation: protein synthesis in virus-infected cells. Cold Spring Harbor Perspect. Biol. *5*, a012351. https://doi.org/10.1101/cshperspect.a012351.

14. Ganem, D. (2010). KSHV and the pathogenesis of Kaposi sarcoma: listening to human biology and medicine. J. Clin. Investig. *120*, 939–949. https://doi.org/10.1172/JCI40567.

15. Dittmer, D.P., and Damania, B. (2019). Kaposi's Sarcoma-Associated Herpesvirus (KSHV)-Associated Disease in the AIDS Patient: An Update. Cancer Treat Res. *177*, 63–80. https://doi.org/10.1007/978-3-030-03502-0_3.

16. Broussard, G., and Damania, B. (2020). Regulation of KSHV Latency and Lytic Reactivation. Viruses *12*, 1034. https://doi.org/10.3390/v12091034.

17. Giffin, L., and Damania, B. (2014). KSHV: pathways to tumorigenesis and persistent infection. Adv. Virus Res. *88*, 111–159. https://doi.org/10.1016/B978-0-12-800098-4.00002-7.

18. Arias, C., Weisburd, B., Stern-Ginossar, N., Mercier, A., Madrid, A.S., Bellare, P., Holdorf, M., Weissman, J.S., and Ganem, D. (2014). KSHV 2.0: a comprehensive annotation of the Kaposi's sarcoma-associated herpesvirus genome using next-generation sequencing reveals novel genomic and functional features. PLoS Pathog. *10*, e1003847. https://doi.org/10.1371/journal.ppat.1003847.

19. Murphy, J.C., Harrington, E.M., Schumann, S., Vasconcelos, E.J.R., Mottram, T.J., Harper, K.L., Aspden, J.L., and Whitehouse, A. (2023). Kaposi's sarcoma-associated herpesvirus induces specialised ribosomes to efficiently translate viral lytic mRNAs. Nat. Commun. *14*, 300. https://doi.org/10.1038/s41467-023-35914-5.

20. Haag, S., Kretschmer, J., and Bohnsack, M.T. (2015). WBSCR22/Merm1 is required for late nuclear pre-ribosomal RNA processing and mediates N7-methylation of G1639 in human 18S rRNA. RNA *21*, 180–187. https://doi.org/10.1261/rna.047910.114.

21. Wurm, J.P., Meyer, B., Bahr, U., Held, M., Frolow, O., Kötter, P., Engels, J.W., Heckel, A., Karas, M., Entian, K.D., and Wöhnert, J. (2010). The ribosome assembly factor Nep1 responsible for Bowen-Conradi syndrome is a pseudouridine-N1-specific methyltransferase. Nucleic Acids Res. *38*, 2387–2398. https://doi.org/10.1093/nar/gkp1189.

22. Meyer, B., Wurm, J.P., Kotter, P., Leisegang, M.S., Schilling, V., Buchhaupt, M., Held, M., Bahr, U., Karas, M., Heckel, A., et al. (2011). The Bowen-Conradi syndrome protein Nep1 (Emg1) has a dual role in eukaryotic ribosome biogenesis, as an essential assembly factor and in the methylation of Psi1191 in yeast 18S rRNA. Nucleic Acids Res. *39*, 1526–1537. https://doi.org/10.1093/nar/gkq931.

23. Cheng, J., Lau, B., Thoms, M., Ameismeier, M., Berninghausen, O., Hurt, E., and Beckmann, R. (2022). The nucleoplasmic phase of pre-40S formation prior to nuclear export. Nucleic Acids Res. *50*, 11924–11937. https://doi.org/10.1093/nar/gkac961.

24. Babaian, A., Rothe, K., Girodat, D., Minia, I., Djondovic, S., Milek, M., Spencer Miko, S.E., Wieden, H.J., Landthaler, M., Morin, G.B., and Mager, D.L. (2020). Loss of m(1)acp(3)Psi Ribosomal RNA Modification Is a Major Feature of Cancer. Cell Rep. *31*, 107611. https://doi.org/10.1016/j.celrep.2020.107611.

25. Johnson, M.C., Ghalei, H., Doxtader, K.A., Karbstein, K., and Stroupe, M.E. (2017). Structural Heterogeneity in Pre-40S Ribosomes. Structure *25*, 329–340. https://doi.org/10.1016/j.str.2016.12.011.

26. Leulliot, N., Bohnsack, M.T., Graille, M., Tollervey, D., and Van Tilbeurgh, H. (2008). The yeast ribosome synthesis factor Emg1 is a novel member of the superfamily of alpha/beta knot fold methyltransferases. Nucleic Acids Res. *36*, 629–639. https://doi.org/10.1093/nar/gkm1074.

27. Armistead, J., Khatkar, S., Meyer, B., Mark, B.L., Patel, N., Coghlan, G., Lamont, R.E., Liu, S., Wiechert, J., Cattini, P.A., et al. (2009). Mutation of a gene essential for ribosome biogenesis, EMG1, causes Bowen-Conradi syndrome. Am. J. Hum. Genet. *84*, 728–739. https://doi.org/10.1016/j.ajhg.2009.04.017.

28. Lowry, R.B., Innes, A.M., Bernier, F.P., McLeod, D.R., Greenberg, C.R., Chudley, A.E., Chodirker, B., Marles, S.L., Crumley, M.J., Loredo-Osti, J.C., et al. (2003). Bowen-Conradi syndrome: a clinical and genetic study. Am. J. Med. Genet. *120A*, 423–428. https://doi.org/10.1002/ajmg.a.20059.

29. Warda, A.S., Freytag, B., Haag, S., Sloan, K.E., Görlich, D., and Bohnsack, M.T. (2016). Effects of the Bowen-Conradi syndrome mutation in EMG1 on its nuclear import, stability and nucleolar recruitment. Hum. Mol. Genet. *25*, 5353–5364. https://doi.org/10.1093/hmg/ddw351.

30. Zhao, Y., Rai, J., Yu, H., and Li, H. (2022). CryoEM structures of pseudouridine-free ribosome suggest impacts of chemical modifications on ribosome conformations. Structure *30*, 983–992. https://doi.org/10.1016/j.str.2022.04.002.

31. Schumann, S., Jackson, B.R., Yule, I., Whitehead, S.K., Revill, C., Foster, R., and Whitehouse, A. (2016). Targeting the ATP-dependent formation of herpesvirus ribonucleoprotein particle assembly as an antiviral approach. Nat. Microbiol. *2*, 16201. https://doi.org/10.1038/nmicrobiol.2016.201.

32. Harper, K.L., Mottram, T.J., Anene, C.A., Foster, B., Patterson, M.R., McDonnell, E., Macdonald, A., Westhead, D., and Whitehouse, A. (2022). Dysregulation of the miR-30c/DLL4 axis by circHIPK3 is essential for KSHV lytic replication. EMBO Rep. *23*, e54117. https://doi.org/10.15252/embr.202154117.

33. Harper, K.L., Harrington, E.M., Hayward, C., Anene, C.A., Wongwiwat, W., White, R.E., and Whitehouse, A. (2024). Virus-modified paraspeckle-like condensates are hubs for viral RNA processing and their formation drives genomic instability. Nat. Commun. *15*, 10240. https://doi.org/10.1038/s41467-024-54592-5.

34. Carden, H., Harper, K.L., Mottram, T.J., Manners, O., Allott, K.L., Dallas, M.L., Hughes, D.J., Lippiat, J.D., Mankouri, J., and Whitehouse, A. (2024). K(v)1.3-induced hyperpolarization is required for efficient Kaposi's sarcoma-associated herpesvirus lytic replication. Sci. Signal. *17*, eadg4124. https://doi.org/10.1126/scisignal.adg4124.

35. Manners, O., Baquero-Perez, B., Mottram, T.J., Yonchev, I.D., Trevelyan, C.J., Harper, K.L., Menezes, S., Patterson, M.R., Macdonald, A., Wilson, S.A., et al. (2023). m(6)A Regulates the Stability of Cellular Transcripts Required for Efficient KSHV Lytic Replication. Viruses *15*, 1381. https://doi.org/10.3390/v15061381.

STAR★METHODS

KEY RESOURCES TABLE

REAGENT or RESOURCE	SOURCE	IDENTIFIER
Antibodies		
EMG1	Proteintech	Cat: #11065-1-AP; RRID: AB_874093
FLAG	Sigma	Cat: #F7425; RRID: AB_439687
es19	Proteintech	Cat: #15085-1-AP; RRID: AB_2180202
GAPDH	Proteintech	Cat: #60004-1-Ig; RRID: AB_2107436
CDK1/cdc2	Abcam	Cat: #ab18; RRID: AB_2074906
Lamin B	Proteintech	Cat: #66095-1-Ig, RRID: AB_11232208
LANA	Sigma	Cat: #MABE1109
ORF65	Cambridge Research Biochemicals	Cat: #crb2005224
ORF26	Novus	Cat: #NBP1-47357, RRID:AB_10010311
K8	Santa Cruz Biotechnology	Cat: #sc-69797, RRID:AB_1124280
ORF57	Santa Cruz Biotechnology	Cat: #sc-135747; RRID: AB_2011973
Chemicals, peptides, and recombinant proteins		
Lipofectamine 2000	Invitrogen	Cat: #10696343
cOmplete™, EDTA-free Protease Inhibitor Cocktail	Sigma-Aldrich	Cat: #11873580001
Hygromycin B	Fisher Scientific (Gibco)	Cat: #10687010
Puromycin	Fisher Scientific (Gibco)	Cat: #12122530
DMEM, high glucose	Fisher Scientific (Gibco)	Cat: #41965062
RPMI 1640 medium	Fisher Scientific (Gibco)	Cat: #21875091
FBS	Fisher Scientific (Gibco)	Cat: #A5256701
Opti-MEM	Fisher Scientific (Gibco)	Cat: #31985070
Penicillin-Streptomycin	Fisher Scientific (Gibco)	Cat: #15070063
Fab-Trap beads	Proteintech	Cat: #ffa-100
GoTaq qPCR MasterMix	Promega	Cat: #A6002
PBS	Fisher Scientific (Gibco)	Cat: #10010001
Triton X-100	Thermofisher	Cat: #FH10
Alexa Fluor 546	Fisher Scientific	Cat: #10789154
Vectashield antifade mounting medium with DAPI	Vector Laboratories	Cat: #H-1200-10
Cyclohexamide	Merck	Cat: #C4859-1ML
Sucrose	Merck millipore	Cat: #107687
Tris-HCl	Invitrogen	Cat: #15567027
NaCl, RNase-free	Thermofisher Scientific	Cat: #AM9760G
MgCl2	Invitrogen	Cat: #10418464
IGEPAL	Thermofisher Scientific	Cat: #15443719
Turbo DNase	Invitrogen	Cat: #10646175
RNasin Plus RNase inhibitor	Promega	Cat: #N2611
12.5 mL Ultraclear tubes	Seton Scientific	Cat:#7031
Ultrascript 2.0	PCR Biosystems	Cat:#PB30.31–10
HinF1	New England Biolabs	Cat:#R0155S
Critical commercial assays		
Monarch Total RNA Miniprep Kit	New England Biosciences	Cat: #T2010S
Lunascript RT Supermix Kit	New England Biosciences	Cat:#E3010L
Click-iT L-azidohomoalanine reaction kit	Thermo Fisher	Cat: #C10102

(*Continued on next page*)

Continued

REAGENT or RESOURCE	SOURCE	IDENTIFIER
DNA blood and tissue extraction kit	Qiagen	Cat: #69504
Luciferase kit	Promega	Cat: #E1910
Experimental models: Cell lines		
Human: TREx-BCBL1-Rta cells	Gift from Professor JU Jung (University of Southern California)	N/A
Human: HEK293T cells	ATCC	N/A
Human: TREx-BCBL1 cells	Gift from A. Hislop (University of Birmingham, UK)	N/A
Oligonucleotides (qPCR)		
EMG1	fwd: CCACCAGAGTTTGCTGATGC	rvs: ATTCGGGTCTGGGGATT
GAPDH	fwd:GTGGTCATGAGTCCTTCCACGAT	rvs: AGGGTCATC ATCTCTGCCCCCTC
ORF57	fwd: GCCATAATCAAGCGTACTG	rvs: GCAGACAAATATTGCGGTGT
ORF65	fwd: AAGGTGAGAGACCCCGTGAT	rvs: TCCAGGGTATTCATGCGAGC
K8	fwd: AGGACCACACATTTCGCAAC	rvs: ACCCCTTGTCAGTTCTTC
ORF26	fwd: TTGTGCTCGAATCCAACGG	rvs: ATGTGCGCCCCATAAATGAC
ORF34	fwd: TGCCCTGAAGTACACCAAGT	rvs: CAGTAGGATTCCACCCACGT
Software and algorithms		
GraphPad Prism 9	GraphPad	https://graphpad.com
ImageJ	National Institutes of Health	https://imagej.net/ij/
Image Studio version 5.2.5	LicorBIO	https://www.licor.com/bio/image-studio
Zen software: blue (2.5 lite) and black	Zeiss	https://www.zeiss.com/microscopy/en/products/software/zeiss-zen.html

EXPERIMENTAL MODEL

Cell culture

TREx-BCBL1-Rta cells, a B cell lymphoma cell line latently infected with KSHV engineered to contain a doxycycline inducible myc-Rta were a gift from Professor JU Jung (University of Southern California). TREx-BCBL1-Rta cells were cultured in RPMI1640 with glutamine (Gibco), supplemented with 10% Fetal Bovine Serum (FBS) (Gibco), 1% P/S (Gibco) and 100 μg/mL hygromycin B (ThermoFisher). Virus lytic replication in TREx-BCBL1-Rta cells was induced via addition of 2 μg/mL doxycycline hyclate (Sigma-Aldrich).[31]

BCBL1 cells were a gift from A. Hislop (University of Birmingham, UK). BCBL1 cells were cultured in the same media conditions as TREx-BCBL1-Rta cells but omitting the hygromycin B. Virus lytic replication in BCBL1 cells was induced with the addition of 2 mM sodium butyrate and 12-*O*-tetradecanoylphorbol 13-acetate (20 ng/mL; both Sigma-Aldrich).[32] HEK293T cells were purchased from the ATCC and cultured in DMEM (Lonza) and supplemented with 10% FBS and 1% P/S. All cell lines were tested negative for mycoplasma.

Plasmid constructs

The packaging plasmids pVSV.G and psPAX2 were a gift from Dr Edwin Chen (University of Westminster, London). EMG1 shRNA constructs were purchased from GE healthcare (KD1 clone ID: TRCN0000134434, KD2 clone ID: V3SVHSHC_8318171). The scr sequence is: CCGCAGGTATGCACGCGT.

METHOD DETAILS

Co-immunoprecipitations

TREx-BCBL-Rta cell lines overexpressing FLAG-2xStrep tagged PNO1 bait protein or a control TREx-BCBL1-Rta cell line were either reactivated or remained latent.[19] After 24 h, cell pellets were resuspended in 1 mL pre-cooled ribosomal lysis buffer (10 mM Tris (pH 7.6), 100 mM KCl, 2 mM $MgCl_2$, 0.5% (v/v) NP-40, 1 mM DTT, 1x protease inhibitor, 1% (v/v) phosphatase inhibitor), kept on ice for 20 min then centrifuged at 5000 *x g* for 12 min at 4°C. FLAG-Trap co-immunoprecipitations were performed as per the manufacturers protocol (Chromotek). Briefly, FLAG-Trap agarose beads (30 μL per sample) were combined with cell lysates, followed by a 2 h incubation at 4 °C with rotation. The beads were washed three times with ribosomal wash buffer (10mM Tris-HCl (pH 7.6), 100 mM KCl, 2 mM $MgCl_2$) and samples were analysed via western blotting.

Strep-Tactin XT coated beads (Cambridge bioscience) (30 μL per sample) were washed with 1 mL lysis buffer (without protease inhibitor, phosphatase inhibitor and DTT) 3 times and combined with BCBL cell lysate that had been reactivated for 24 h, or harbored latent KSHV overnight at 4°C with rotation. Samples were washed 3 times with pre-cooled ribosomal wash buffer 1 (10mM Tris-HCl (pH 7.6), 100 mM KCl, 2 mM $MgCl_2$) and once with pre-cooled ribosomal wash buffer 2 (10 mM Tris-HCl (pH 7.6), 2 mM $MgCl_2$) then analysed via western blotting.

Immunoblotting

Cell lysates were separated using 8–12% polyacrylamide gels and transferred to Amersham Nitrocellulose Membranes (GE healthcare) via *Trans*-blot Turbo Transfer system (Bio-Rad). Membranes were blocked in TBS +0.1% tween with 5% (w/v) dried skimmed milk powder. Membranes were probed with appropriate primary antibodies and Dylight800 and 600 secondary antibodies at 1/10000 dilution (ThermoFisher). Proteins were detected using the LICOR.

RNA extraction and qPCR

Total RNA was extracted using Monarch Total RNA Miniprep Kit (NEB) as per manufacturer's protocol. 1 μg RNA was reverse transcribed using LunaScript RT SuperMix Kit (NEB). qPCR was performed using synthesised cDNA, GoTaq qPCR MasterMix (Promega) and the appropriate primer. qPCR was performed on Rotorgene Q and analyzed by the ΔΔCT method against a housekeeping gene as previously described before plotting as fold.[33]

Aminocarboxyl propyl reverse transcription (aRT)-PCR assay

Levels of 18S.1248m1acp3Ψ modification were measured by aRT-PCR as outlined in Babain et al., 2020 which provides comprehensive experimental evidence that the technique is both reproducible and quantitative within the cycles stated. Briefly, RNA was isolated from cell lysates via TRIZOl extraction, or from 40S subunits via polysome profiling. An RT reaction (50°C for 30 min, 95°C for 10 min) was carried out on 220 ng total RNA with Ultrascript 2.0 (PB30.31-10, Invitrogen) using random hexamers. An aliquot of 1 μL of cDNA product (pre-diluted 1/5) was used as a template for PCR (94°C for 5 min, 25 cycles [94°C for 30 s, 55°C for 30 s, 72°C for 30 s], 72°C for 7 min) and 5 μL of PCR amplification product was used for HinF1 digestion (NEB). For each sample two technical repeats of HinF1 digestion were carried out and digested samples were run on a 2% agarose gel at 80V for 1hour.

Lentiviral expression and shRNA constructs

Lentiviruses were generated by transfection of HEK293T cells using two packaging plasmids pPAX.2 and pVSV-G, a gift from Dr Edwin Chen (University of Westminster). Per 12-well, 4 μL of lipofectamine 2000 (Thermo Scientific) were used together with 1.2 μg of pLKO.1 plasmid expressing shRNA against the protein of interest, 0.65 μg of pVSV.G, and 0.65 μg psPAX2. Eight hours post-transfection, media was changed with 1.5 mL of DMEM supplemented with 10% (v/v) FCS. Two days post-transfection, viral supernatants were harvested, filtered through a 0.45 μm filter (Merck Millipore) and immediately used for transductions of TREx-BCBL1-Rta cells. Cells (500,000) in 12 well plates were infected by spin inoculation for 60 min at 800 x g at room temperature, in the presence of 8 μg/mL of polybrene (Merck Millipore). 3 μg/mL Puromycin (Gibco) was added 48 h after transduction before knockdown analyzed via qPCR and western blot if appropriate.[34]

Global translation assay

TREx-BCBL1-Rta cells stably expressing scrambled shRNA or shRNAs targeting EMG1 were seeded into a 6-well plate at 1×10^6 cells/well with 2 mL RPMI selection media without methionine, which was chased out over 1 hr. Cells were treated with Click-iT L-azidohomoalanine (AHA, 40 μM, Thermo Fisher) for 3 hrs, then washed in 1x PBS and fixed in PBS containing 4% (v/v) paraformaldehyde for 15 min. Cells were again washed in 1x PBS and permeabilised using 1x PBS containing 0.25% Triton X-100 for 15 min. AHA was stained with a Click-iT reaction kit (Thermo Fisher) using an alkyne Alexa Fluor 488, 1 μM, as described by the manufacturer. Finally, cells were washed in PBS containing 1% BSA and resuspended in PBS containing 0.5% BSA before fluorescence quantification by CytoFlex S Benchtop Flow Cytometer (Beckman Coulter).

Viral load and reinfection assays

TREx-BCBL1-Rta cells stably expressing scrambled shRNA or shRNAs targeting EMG1 were seeded in 2 mL of fresh RPMI media (300,000 cells/mL) without puromycin into a 6-well plate. Lytic replication was induced by adding doxycycline (2 μg/mL) for 72 h, with one scr well left uninduced as a control. Cell pellets were centrifuged at 500 *x g* for 5 min at 4°C and the pellet was collected for DNA extraction. The supernatant, containing any released virion particles, was added in a 1:1, 1:0.5 or 1:0.1 ratio to HEK293T cells seeded in the wells of 6-well plates at 50% confluency. The cells were incubated for 48 h, then harvested and DNA and RNA was isolated from the cell pellets. Purified RNA was reverse transcribed, and RNA and DNA samples analyzed by qPCR for the levels of *ORF57* to determine genome levels and infectious virion production.[35]

Immunofluorescence

Viral supernatant produced from viral reinfection assays were added to HEK293T cells grown on sterilised glass coverslips and incubated for 48 h. The cells were fixed in PBS containing 4% paraformaldehyde (v/v) for 15 min, then permeabilised in PBS containing

1% Triton X-100 for 15 min. All the following steps were incubated for 1 h at 37°C. Coverslips were blocked in PBS containing 1% BSA, incubated in anti-LANA (1/50), then incubated in Alexa Fluor 546 (1/500) before being mounted onto slides using Vectashield hardset mounting medium containing DAPI. Slides were visualised on a Zeiss LSM880 laser scanning confocal microscope and processed using ZEN 2009 imaging software.

Polysome profiling

TREx-BCBL1-Rta cells expressing scr shRNA or EMG1 specific shRNAs were treated with cycloheximide (Sigma) at 100 μg/mL for 3 min at room temperature. A total of ~50 × 10^6 cells were pelleted and washed (1 x PBS) then lysed in ice-cold buffer [50 mM Tris-HCl pH8, 150 mM NaCl, 10 mM MgCl2, 1 mM DTT, 1% IGEPAL, 100 μg/mL cycloheximide, Turbo DNase 24 U/mL (Invitrogen), RNasin Plus RNase Inhibitor 90 U (Promega), 1 × protease inhibitor cocktail (Roche)] for 45 min. Lysates were clarified by centrifugation (12,000 × *g*, 10 min, 4 °C) and the resulting supernatants applied to 5–45% continuous sucrose gradients (10 mM MgCl2, 50 mM Tris-HCl (pH 7.6), 150 mM NaCl, 1 mM DTT and 1× protease inhibitor cocktail). Gradients were then subjected to ultracentrifugation (160,000 × *g*, 3 hrs, 4 °C) in SW-40 rotor. Fractions from each gradient were collected using a Gradient Fractionator (BioComp) and the RNA profile was measured by absorbance (254 nm) across the gradient in real time using an EM-1 Econo UV Monitor (Bio-Rad). All fractions with large polysomes, 3 or more ribosomes per mRNA, were pooled and precipitated [0.3M NaCl, 50% isopropanol] overnight at −80°C. Pellets were washed in 70% ethanol twice, left to air dry, then pooled and resuspended in nuclease-free water. Samples were analyzed by qPCR or aRT-PCR assay.

Luciferase assays

Luciferase activity was detected using the Dual-Luciferase Reporter Assay System (Promega). The 5′ UTR of ORF28 (Sequence ID: MZ712175.1, range: 49031–49090), ORF34 (Sequence ID: OR829374.1, range: 54523–54634) and ORF69 (Sequence ID: MK876733.1, range: 116073–116300) was cloned upstream of the renilla reporter gene in the psiCHECK-2 vector dual-promoter construct, with a control firefly reporter gene on a separate promoter. HEK293T cell lines stably expressing a scr shRNA or EMG1 shRNA plasmid and either a control or EMG1 mutant or wild type EMG1 overexpression construct were seeded in triplicate in 12-well culture plates (Thermo Fisher) at a density of 3 × 10^5 cells per well and grown for 24 h. Cells were transfected with 100 ng of respective plasmids (diluted in 100 μL Opti-mem) using 3 μL Lipofectamine 2000 (InvitrogenTM; diluted in 100 μL Opti-mem) and incubated for a further 24 h. Media was removed from the wells and cells washed gently with 100 μL PBS. Aliquots (100 μL) of 1x passive lysis buffer were added to the cell monolayers and rocked for 20 min at room temperature and then 10 μL of each lysate was transferred to tissue culture treated white microplates (Greiner Bio-One). Luciferase measurements were carried out using a FLUOstar Optima microplate reader (BMG Labtech Ltd), with injectors 1 and 2 being used to dispense 50 μL of Luciferase Assay Reagent II and Stop & Glo Reagent respectively. Renilla luciferase activity was normalized to Firefly luciferase activity.

QUANTIFICATION AND STATISTICAL ANALYSIS

Unless otherwise stated, graphical data shown represent mean ± standard deviation of mean (SD) using three biologically independent experiments. Differences between means were analyzed by unpaired Student's t test or one way analysis of variance (ANOVA) calculated using Graphpad Prism 9 calculator and stated in the figure legend. Statistics were considered significant at $p < 0.05$, with $^{*}p < 0.05$, $^{**}p < 0.01$, $^{***}p < 0.001$ and $^{****}p < 0.0001$.